B

	irradiated leg (Femur&Tibia)	Iliac (behind the lead plate)	non-irradiated organs (away from the lead plate)
Value read on electrometer	5.6 Gy	0.707 Gy	0.056 Gy
Corrected value	5.49 Gy	0.694 Gy	0.052 Gy

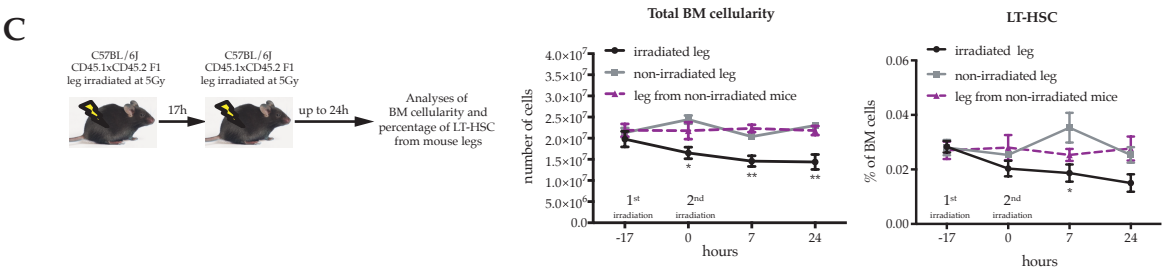

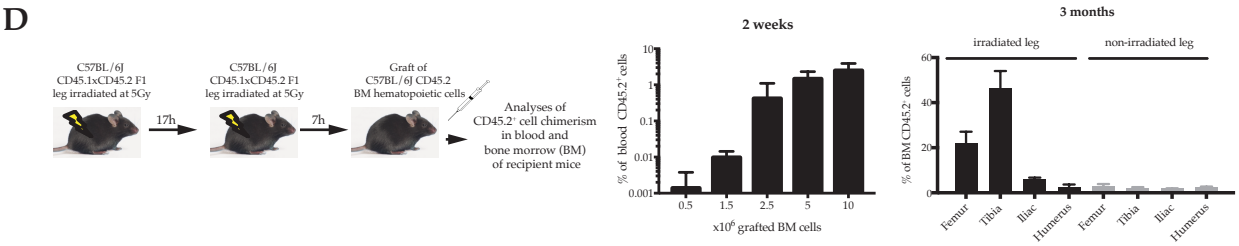

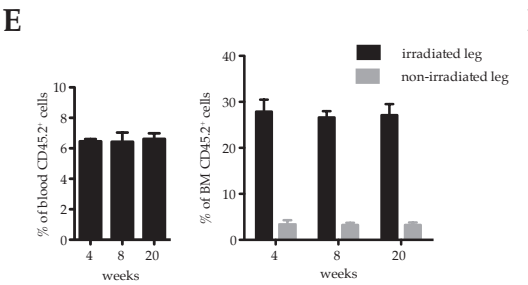

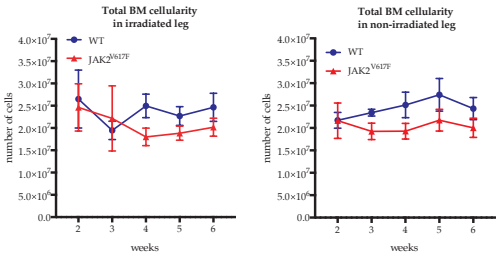

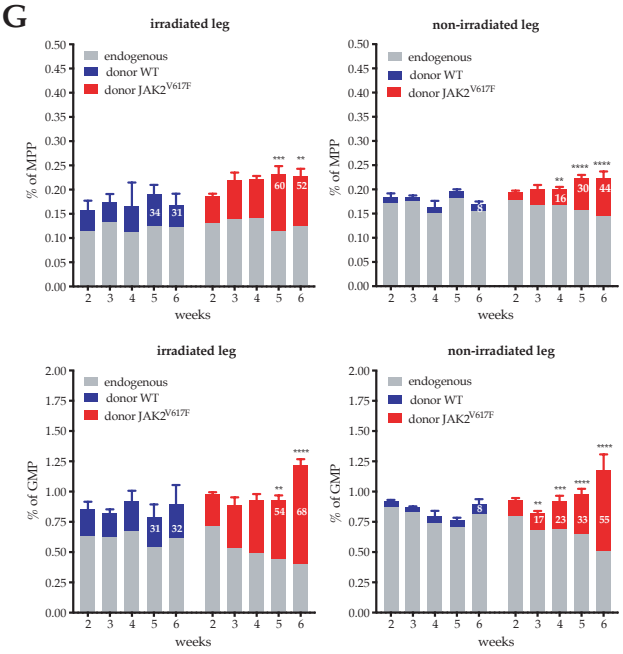

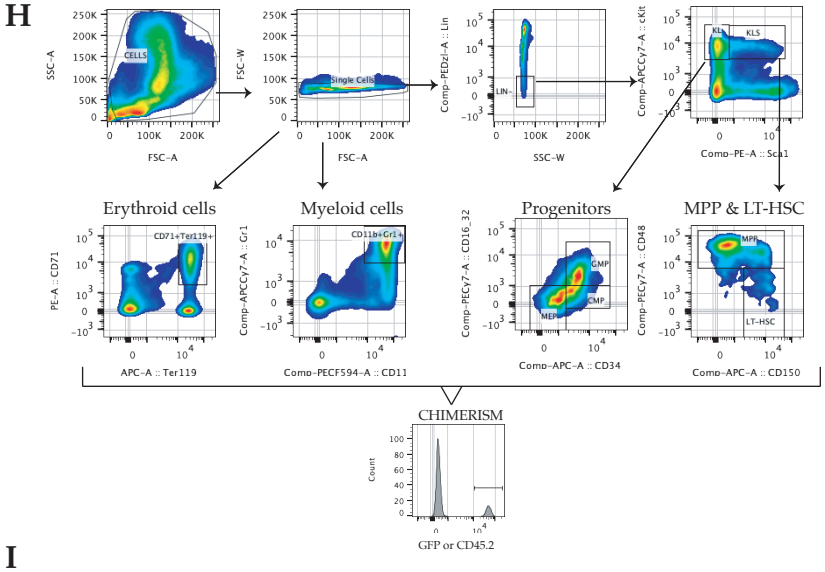

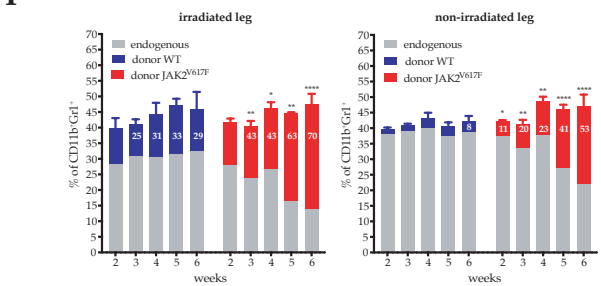

Supplementary Fig. S1: Follow up of Polycythemia Vera development in mice.

A) Irradiation box design (left) and phantom detectors mimetic tissue in the irradiation box (right). **B**) Values of measured irradiation in the irradiated leg (femur and tibia), the iliac bone and non-irradiated organs after irradiation of a single leg with the GSRD1 irradiator. **C**) Experimental design (left), kinetics of bone marrow (BM) cellularity (middle) and of long-term hematopoietic stem cells (LT-HSC) (right) in the irradiated and non-irradiated legs after sequential irradiation (5 Gy 2x with 17 hours rest) of a single mouse leg. **D**) Experimental design (left), percentages of donor $CD45.2^+$ hematopoietic cells detected in blood 2 weeks after grafting donor BM cells into a single irradiated leg of $CD45.1^+/CD45.2^+$ recipient mice (middle). X axis refers to varying number of grafted cells. Percentages of donor-derived $CD45.2^+$ hematopoietic cells detected in BM of the indicated site 3 months after transplantation of 10^7 donor cells into a single irradiated leg of $CD45.1^+/CD45.2^+$ recipient mice (right). **E)** After transplantation of WT BM cells in a single irradiated leg, kinetics of peripheral blood cells (left) and of contribution of transplanted WT BM cells to total BM hematopoietic cells in the irradiated and non-irradiated legs (right). **F**) Kinetics of bone marrow (BM) cellularity in the irradiated (left) and the non-irradiated leg (right) of mice transplanted with $JAK2^{V617F}$ or WT BM cells in a single irradiated leg. **G**) Kinetics of WT or $JAK2^{V617F}$ cell contribution to the multipotent progenitor (MPP) (top) and granulocyte-monocyte progenitor (GMP) (bottom) compartments. **H)** Gating strategies to study, by flow cytometry, chimerism (GFP or CD45.2) in mature erythroid ($CD71^+Ter119^+$) and myeloid cells ($CD11b^+Gr1^+$), progenitors (MEP: $Lin^-cKit^+Sca^-CD16/32^-CD34^-$, CMP: $Lin^-cKit^+Sca^-CD16/32^{low}CD34^+$, GMP: $Lin^-cKit^+Sca^-CD16/32^+CD34^+$), multipotent progenitors (MPP: $Lin^-cKit^+Sca^+CD48^+$) and long-term hematopoietic stem cells (LT-HSC: $Lin^-cKit^+Sca^+CD48^-CD150^+$). **I**) Kinetics of WT or $JAK2^{V617F}$ cell contribution to the mature myeloid ($CD11b^+Gr1^+$) compartment.

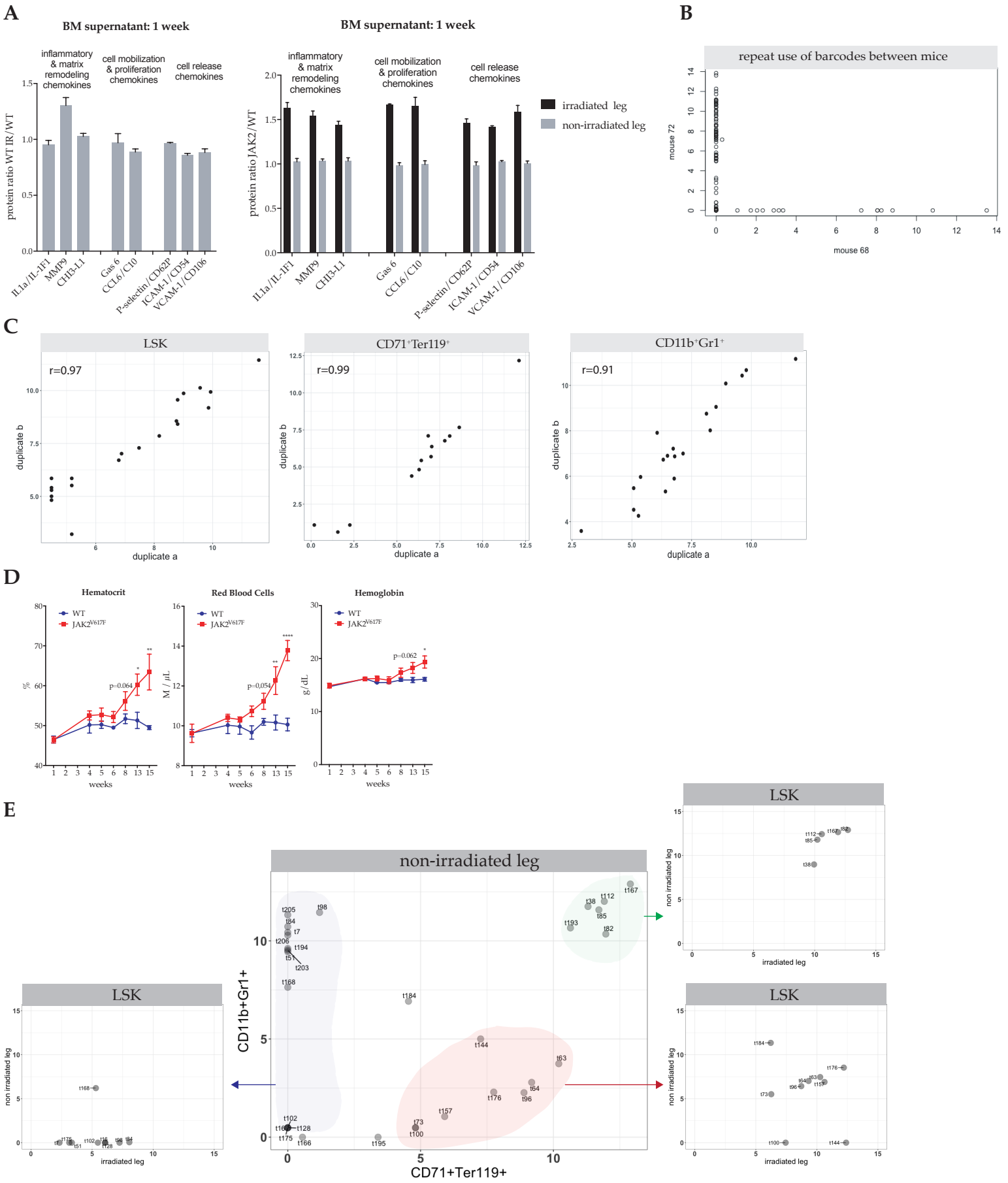

Supplementary Fig. S2: JAK2^{V617F} LSK from irradiated leg colonize the non-irradiated leg.

A) Ratio of chemokine levels in BM supernatants from irradiated and non-irradiated legs ($WT_{irr}/WT_{non\text{-}irr}$) from mice transplanted with WT BM cells (left) and from mice transplanted with JAK2^{V617F} *versus* WT BM cells (right) at 1 week. **B)** Quality controls for accuracy of the inferred chance of having different clones with the same barcode in one mouse (repeat use), by comparing barcode content in two mice that received JAK2^{V617F} LSK from the same transduction batch. **C)** Quality controls for accuracy of barcode detection in LSK cells (left), in CD71^{+}Ter119^{+} erythroid cells (middle) and in CD11b^{+}Gr1^{+} myeloid cells (right) in the two PCR duplicates. **D)** Kinetics of blood parameters after transplantation of 10^5 JAK2^{V617F} or WT LSK cells in single irradiated leg mice. **E)** Barcode frequency in CD71^{+}Ter119^{+} erythroid clones (X axis) and CD11b^{+}Gr1^{+} myeloid clones (Y axis) in non-irradiated leg (middle panel). Barcode frequency in LSK clones between irradiated and non-irradiated legs was assessed for three kinds of barcodes (colorized ROI): barcoded clones mostly present in CD11b^{+}Gr1^{+} myeloid cells (left, purple region), barcoded clones with a higher representation in CD71^{+}Ter119^{+} erythroid cells than CD11b^{+}Gr1^{+} myeloid cells (lower right, pink region), barcoded clones equally represented in CD71^{+}Ter119^{+} erythroid cells and in CD11b^{+}Gr1^{+} myeloid cells (upper right, green region).

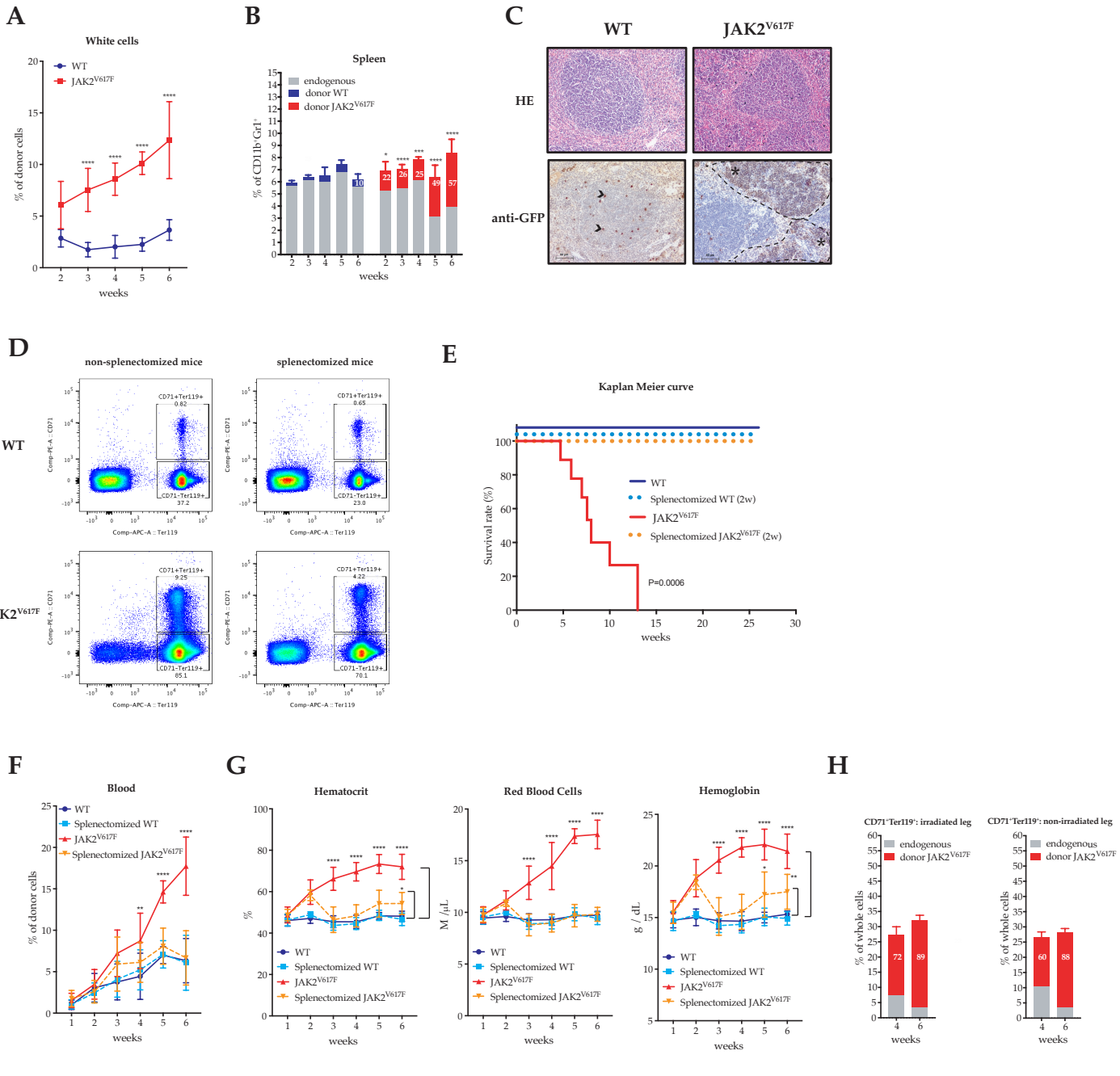

Supplementary Fig. S3: The spleen is necessary for PV development through amplification of the JAK2^{V617F} erythroid compartment.

A) Kinetics of splenic white blood cells in single-leg-irradiated mice transplanted with JAK2^{V617F} or WT BM cells. **B)** Kinetics of WT or JAK2^{V617F} cell contribution to the mature myeloid (CD11b^{+}Gr1^{+}) compartment. **C**) Hematoxylin/Eosin (HE) coloration and anti-GFP labeling (indicating by arrow or * when area of spleen are labelled) of spleen from mice 1 week (time of splenectomy) after transplantation of JAK2^{V617F} or WT BM cells (40x magnification). **D**) Cytometric analysis of erythroid cell compartments of liver from single-leg-irradiated mice 10 weeks after splenectomy. **E)** Survival curve of mice with or without splenectomy two weeks after transplantation of JAK2^{V617F} or WT BM cells. **F**) Kinetics of blood cell chimerism in single-leg-irradiated mice with or without splenectomy two weeks after transplantation of JAK2^{V617F} or WT BM cells. **G)** Kinetics of red blood cell parameters in single-leg-irradiated mice with or without splenectomy two weeks after transplantation JAK2^{V617F} or WT BM cells. **H)** JAK2^{V617F} cell contribution to the CD71^{+}Ter119^{+} compartment in irradiated and non-irradiated legs of mice splenectomized 2 weeks after transplantation of JAK2^{V617F} or WT BM cells.

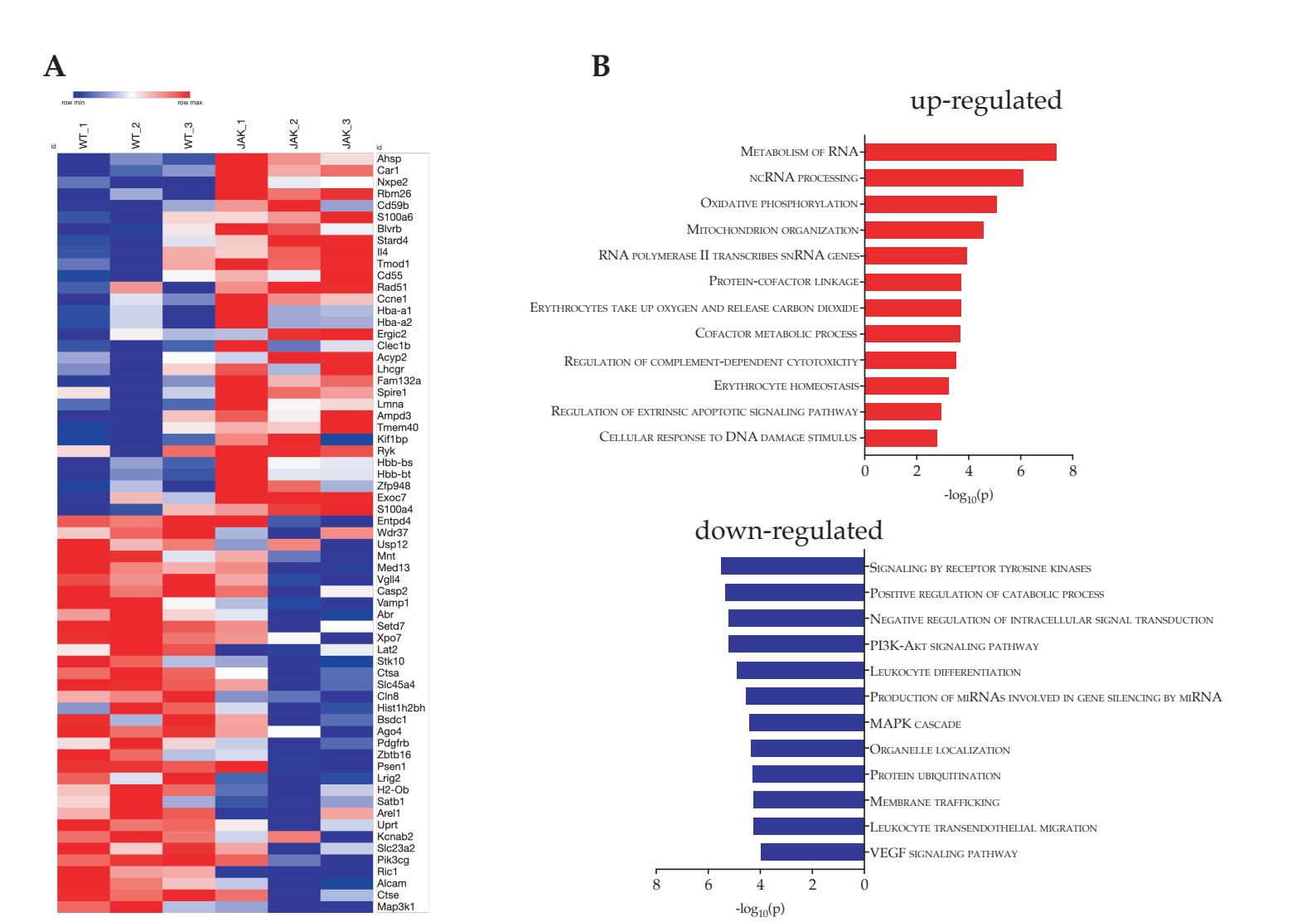

Supplementary Fig. S4: Transcriptome analysis of JAK2^{V617F} HSPC and endogenous HSPC from the non-irradiated leg.

A) Heatmap of differentially expressed genes between endogenous WT and JAK2^{V617F} sorted HSPC from the non-irradiated leg (adjusted P value<0.05, fold change>5 or <-5). **B)** Gene set enrichment of up-regulated and down-regulated pathways in JAK2^{V617F} HSPC compared to WT endogenous HSPC (P value<0.01, n=3 biological replicates per group). **C)** Gene set enrichment analyses showing significant alterations in gene sets involved in oxidative phosphorylation, oxygen up-take and carbon dioxide release and signaling by receptor tyrosine kinases.

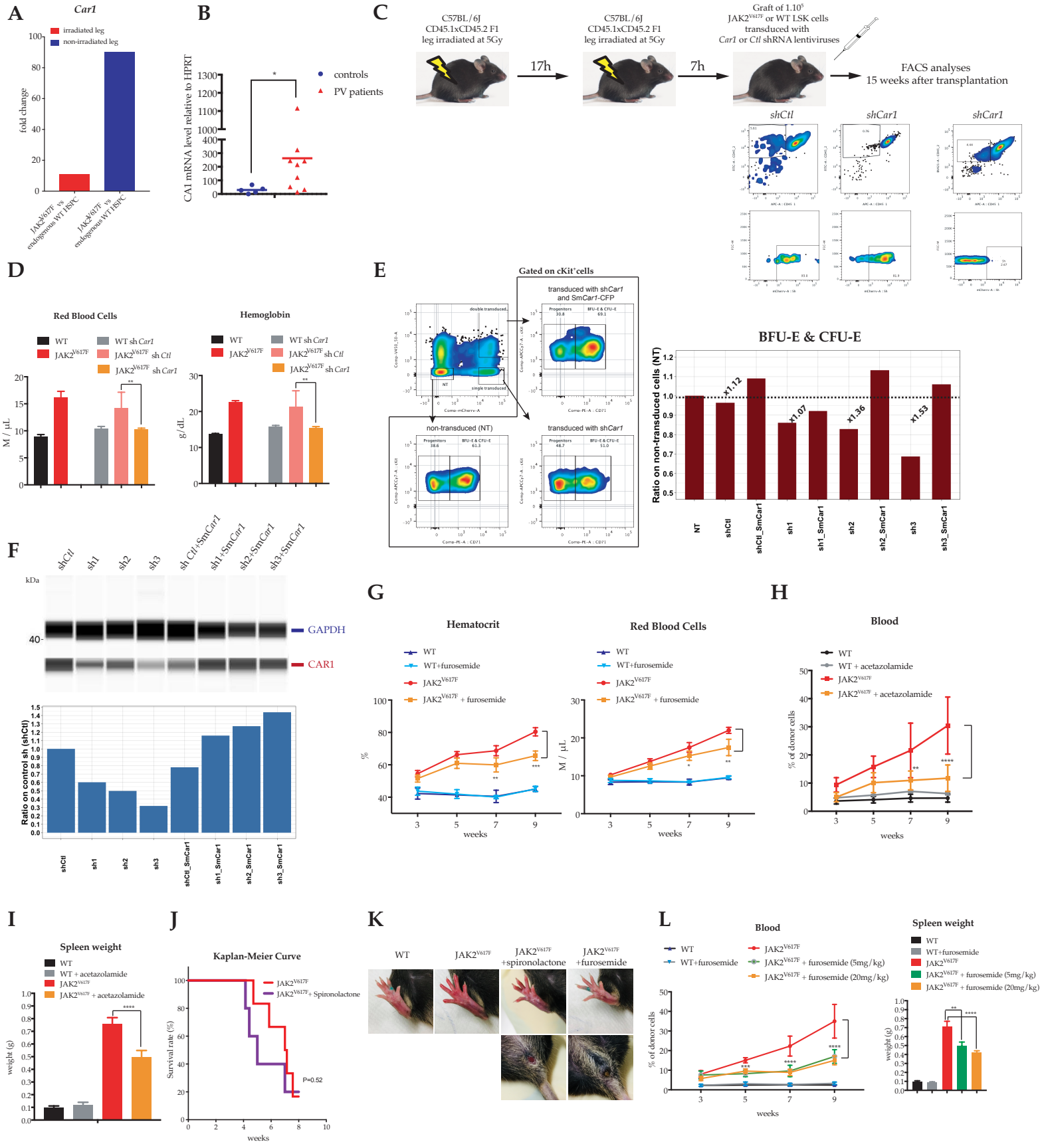

Supplementary Fig. S5: Inhibition of carbonic anhydrase 1 suppresses Polycythemia Vera progression.

A) Fold change of *carbonic anhydrase 1* (*Car1*) mRNA levels in JAK2^{V617F} *versus* endogenous WT HSPC in irradiated and non-irradiated legs from the transcriptomic analysis. **B**) Relative mRNA levels of carbonic anhydrase 1 in CD34^{+} cells from PV patients. **C)** Experimental design of single-leg-irradiated mice transplanted with JAK2^{V617F} or WT LSK cells transduced with *Car1* or *Ctl* shRNA lentivirus that can also express the mCherry gene under H1 promoter (top). FACS analyses of blood chimerism (middle) and mCherry protein expression (bottom) in blood cells from mice transplanted with JAK2^{V617F} LSK cells transduced with lentivirus expressing sh*Ctl* (left panels) or sh*Car1* (middle and right panels). Middle and right panels represent mice transplanted with JAK2^{V617F} LSK cells transduced with sh*Car1* lentivirus and that, based on the detection of mCherry fluorescence, expressed (middle) or not (right) sh*Car1*. **D**) Hematocrit and hemoglobin blood parameters in mice transplanted with JAK2^{V617F} or WT LSK cells transduced with *Car1* or *Ctl* shRNA lentivirus in a single leg irradiated mice. **E)** JAK2^{V617F} Lin^{-}cKit^{+} cells from BM of single-leg-irradiated mice transplanted with JAK2^{V617F} BM cells were co-transduced with a lentivirus expressing control sh (sh*Ctl)* or sh 1 or sh2 or sh3 that targets *Car1* mRNA and a lentivirus expressing a wild type CAR1 from a *Car1* cDNA containing neutral mutations that impair the action of sh1, sh2 and sh3 (Sm*Car1*). These transduced cells were cultured in erythroid medium conditions. (left) FACS analysis strategy to analyse the erythroid differentiation of the JAK2^{V617F} Lin^{-}cKit^{+} cells and (right) ratio on non-transduced cells (NT) of single transduced (sh*Ctl*, sh1, sh2, sh3) or double transduced (sh*Ctl*+Sm*Car1*, sh1+Sm*Car1*, sh2+Sm*Car1*, sh3+Sm*Car1*) cKit^{+}CD71^{+} BFU-E/CFU-E cells in each culture. **F**) Western blot analysis of CAR1 and GAPDH proteins in the different JAK2^{V617F} Lin^{-} cells studied in **E** (up) and relative CAR1 expression in these JAK2^{V617F} Lin^{-} cells compared to CAR1 expression level in cells transduced with shCtl (bottom). **G**) Hematocrit and red blood cell count from single-leg-irradiated mice transplanted with JAK2^{V617F} or WT BM cells and treated daily (or not) with furosemide beginning 2 weeks after transplantation. **H**) Kinetics of blood chimerism in micetransplanted with JAK2^{V617F} or WT BM cells and daily treated or not with acetazolamide starting two weeks after transplantation. **I**) Spleen weight 8 weeks after the beginning of acetazolamide treatment. **J)** Survival curve of single-leg-irradiated mice transplanted with JAK2^{V617F} BM cells and treated daily (or not) with spironolactone beginning 2 weeks after transplantation. **K)** Pictures show redness in feet (top) and anal bleeding (bottom) in mice transplanted with WT or JAK2^{V617F} BM cells not treated (two left pictures) or treated daily with spironolactone (middle) or furosemide (right) for 5 weeks. **L**) (left) Kinetics of blood chimerism and (right) spleen weight in mice transplanted with JAK2^{V617F} or WT BM cells and daily treated or not with 5 or 20mg/kg of furosemide starting two weeks after transplantation.